LIGHT-BY-LIGHT SCATTERING IN ULTRAPERIPHERAL HEAVY-ION COLLISIONS — NEW POSSIBILITIES*

Antoni Szczurek[a,b], Pawel Jucha[a]

[a]Institute of Nuclear Physics Polish Academy of Sciences, Kraków, Poland
[b]University of Rzeszów, 35-310 Rzeszów, Poland

Received 17 December 2024, accepted 29 January 2025, published online 10 April 2025

Light-by-light scattering is a relatively new area of experimental physics. Our recent, theoretical research shows that studying two-photon measurements in regions with lower transverse momentum ($p_{t,\gamma}$) and invariant mass ($M_{\gamma\gamma}$) allows us to observe not only the main contribution of photon scattering, known as fermionic loops but also mechanisms like the VDM-Regge (double-photon hadronic fluctuation). In addition, diphoton measurements at low diphoton masses are crucial for studies of light-meson resonance contributions in $\gamma\gamma \to \gamma\gamma$ scattering. We also focus on the interference between different contributions. For future experiments with the ALICE FoCal and ALICE-3 detectors, we have calculated background contamination and have explored possibilities to minimize their impact.

DOI:10.5506/APhysPolBSupp.18.2-A37

1. Introduction

Light-by-light scattering, a quantum electrodynamic process where two photons interact and scatter off each other, is a phenomenon observed for the first time at the Large Hadron Collider (LHC) in 2017 [1]. Light-by-light scattering can be observed due to the intense electromagnetic fields generated by the ultrarelativistic nuclei. These fields can be considered as a flux of quasi-real photons that surround the ions. When two ions pass by each other, these electromagnetic fields can interact, enabling the light-by-light scattering. In ultraperipheral collisions, the process is essentially free of unwanted backgrounds.

Recent experiments at the LHC, conducted by the CMS [2] and ATLAS [3] collaborations, have successfully observed and measured light-by-light scattering in heavy-ion collisions. However, both experiments use rather high thresholds for diphoton mass (5 GeV) and transverse momentum (2 GeV

* Presented by A. Szczurek at the 57$^{\text{th}}$ Zakopane Conference on Nuclear Physics, *Extremes of the Nuclear Landscape*, Zakopane, Poland, 25 August–1 September, 2024.

for CMS, and 2.5 GeV for ATLAS). The goal of our latest study [4] was to make predictions for future experiments with a lower threshold. Also, the study for different mechanisms, such as VDM-Regge or light meson resonances, was conducted, searching for possibilities of their observation or even measurement.

2. Sketch of the formalism

The Equivalent Photon Approximation [5] relies on the knowledge about elementary cross section as a function of diphoton mass $W_{\gamma\gamma}$ and distributions in the scattering angle, $z = \cos\theta$. In this paper, various mechanisms of $\gamma\gamma \to \gamma\gamma$ process are taken into consideration. The most common contribution is due to the four-vertex fermionic loops, so-called boxes, presented in Fig. 1 (a). The calculation based on Feynman diagrams was carried out using FormCalc and LoopTools libraries based on Mathematica software [6]. To designate the cross sections for unpolarized photons, 16 photon helicity combinations of the amplitude must be added up

$$\sum_{\lambda_1,\lambda_2,\lambda_3,\lambda_4} \left|\mathcal{A}^{\gamma\gamma\to\gamma\gamma}_{\lambda_1\lambda_2\to\lambda_3\lambda_4}\right|^2 = 2\left|\mathcal{A}_{++++}\right|^2 + 2\left|\mathcal{A}_{+--+}\right|^2 + 2\left|\mathcal{A}_{+-+-}\right|^2 + 2\left|\mathcal{A}_{++--}\right|^2 + 8\left|\mathcal{A}_{+-++}\right|^2 . \quad (1)$$

Another mechanism of light-by-light scattering is double-photon hadronic fluctuation (Fig. 1 (b)). The mathematical description of the VDM-Regge mechanisms was presented in [7]

$$\mathcal{A} = \Sigma_{i,j} C_i^2 C_j^2 \left(C_{\mathbb{P}} \left(\frac{s}{s_0}\right)^{\alpha_{\mathbb{P}}(t)-1} F(t) + C_{\mathbb{R}} \left(\frac{s}{s_0}\right)^{\alpha_{\mathbb{R}}(t)-1} F(t) \right) + \Sigma_{i,j} C_i^2 C_j^2 \left(C_{\mathbb{P}} \left(\frac{s}{s_0}\right)^{\alpha_{\mathbb{P}}(u)-1} F(u) + C_{\mathbb{R}} \left(\frac{s}{s_0}\right)^{\alpha_{\mathbb{R}}(u)-1} F(u) \right) . \quad (2)$$

The light-meson resonances (Fig. 1 (c)) such as π, η, and η' in $\gamma\gamma \to \gamma\gamma$ scattering are described using the relativistic Breit–Wigner formula presented in [8]

$$\mathcal{A}_{\gamma\gamma\to R\to\gamma\gamma}(\lambda_1,\lambda_2) = \frac{\sqrt{64\pi^2 W_{\gamma\gamma}^2 \Gamma_R^2 Br^2(R\to\gamma\gamma)}}{\hat{s} - m_R^2 - i m_R \Gamma_R} \times \frac{1}{\sqrt{2\pi}} \delta_{\lambda_1-\lambda_2} , \quad (3)$$

In the case of two-photon measurement, the production of four photons from the $\pi^0\pi^0$ decay (Fig. 1 (d)), where only two photons are observed in detectors, constitutes the main background. Based on [9], the idea of how to reduce the background is discussed below.

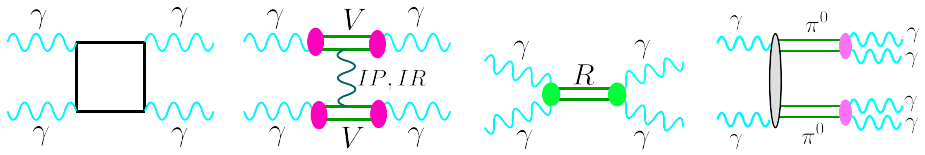

Fig. 1. Feynman diagrams of the LbL scattering mechanisms: (a) fermionic loops, (b) VDM-Regge, (c) low-mass resonances in the s-channel, (d) two-π^0 background.

The calculation of nuclear cross section for light-by-light scattering is performed with the help of the equivalent photon formula in the impact parameter space

$$\frac{\mathrm{d}\sigma(\mathrm{PbPb}\to\mathrm{PbPb}\gamma\gamma)}{\mathrm{d}y_{\gamma_1}\,\mathrm{d}y_{\gamma_2}\,\mathrm{d}p_{\mathrm{t},\gamma}} = \int \frac{\mathrm{d}\sigma_{\gamma\gamma\to\gamma\gamma}(W_{\gamma\gamma})}{\mathrm{d}z} N(\omega_1,b_1)N(\omega_2,b_2)S^2(b) \times \mathrm{d}^2b\,\mathrm{d}\bar{b}_x\,\mathrm{d}\bar{b}_y \frac{W_{\gamma\gamma}}{2}\frac{\mathrm{d}W_{\gamma\gamma}\,\mathrm{d}Y_{\gamma\gamma}}{\mathrm{d}y_{\gamma_1}\,\mathrm{d}y_{\gamma_2}\,\mathrm{d}p_{\mathrm{t},\gamma}}\,\mathrm{d}z\,. \tag{4}$$

Here, the $\sigma_{\gamma\gamma\to\gamma\gamma}(W_{\gamma\gamma})$ is the elementary cross section, $Y_{\gamma\gamma}$ is the rapidity of outgoing two photons, and $\bar{b}_x$, $\bar{b}_y$ are the components of the vector $(\vec{b}_1+\vec{b}_2)/2$, where $\vec{b}=\vec{b}_1-\vec{b}_2$. Above, $z=\cos\theta$. The $N(\omega_i,b_i)$ is photon flux, which is obtained from charge distribution in the nucleus. The $S^2(b)$ denotes the survival factor. In our recent studies, the sharp edge formula ($S^2(b)=\Theta(b-b_{\mathrm{max}})$) was replaced by the formula

$$S^2(b)=\exp\left(-\sigma_{NN}T_{AA}(b)\right)\,, \tag{5}$$

where σ_{NN} is the nucleon–nucleon interaction cross section, and $T_{AA}(b)$ is related to the so-called nuclear thickness function [4].

3. Results for $\gamma\gamma\to\gamma\gamma$ collisions

Calculations of the elementary cross section for light-by-light scattering show that in a diphoton energy region below 1 GeV, one can expect a significant signal from the loop contribution. Figure 2 (a) displays separate contributions for different fermions in the loop. In Fig. 2 (b), the ratio of different contributions to the total cross section is presented. Here, the importance of interference is illustrated. The incoherent sum between quarkish and leptonic loops cannot sum up to 1. The impact of interference is estimated to be around 20%.

The analysis of interference of box and VDM-Regge mechanisms was also conducted. In Fig. 3, we show the plots of ratios of the sum of two contributions (VDM-Regge, boxes) to the box contributions as a function

of $z = \cos\theta$ variable. The role of interference is clearly visible for $|z| \to 1$. The smaller the scattering angle, the greater the impact of the VDM-Regge contribution on the cross section. We found that the effect of interference is destructive.

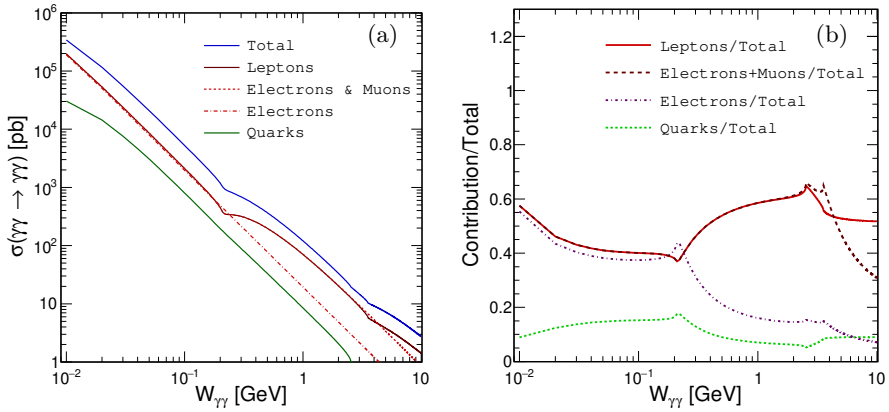

Fig. 2. (Colour on-line) (a) Elementary cross section (in pb) as a function of energy. The total cross section (blue/black solid line) is split somewhat artificially into quarks (green/grey solid line), electrons (red/light grey dashed line), electrons and muons (red/light grey dotted line), and leptons (red/light grey solid line) contributions; (b) Ratio of each contribution to a coherent sum of them: leptonic cross section divided by the total cross section (red/light grey solid line), quarks (green dotted line), electrons (magenta dash–dotted line), and the sum of electron and muon contributions (dashed dark red/black line).

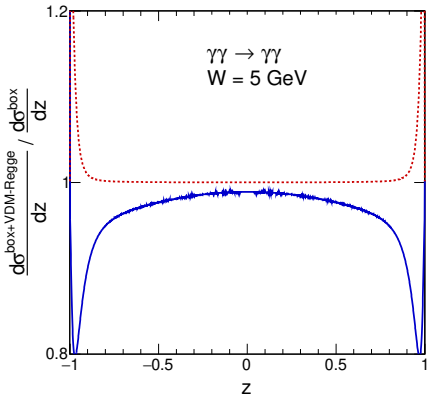

Fig. 3. (Colour on-line) The ratio of the coherent (blue/black) and incoherent (red/grey) sum of the box and VDM-Regge contributions divided by the cross section for the box contribution alone for $W_{\gamma\gamma} = 5$ GeV.

4. Results for nuclear collisions

In Fig. 4 (a), the distribution of diphoton invariant mass for ATLAS kinematical cuts with sharp edge of nucleus and the survival factor based on Eq. (5) is presented. All theoretical approaches, including SuperChic, underestimate the cross section in the low-mass region. In Fig. 4 (b), the ratio of results for both our approaches for the impact parameter cutoff is shown. The difference is changing between 4% for smaller values of the diphoton mass up to 10% for higher masses.

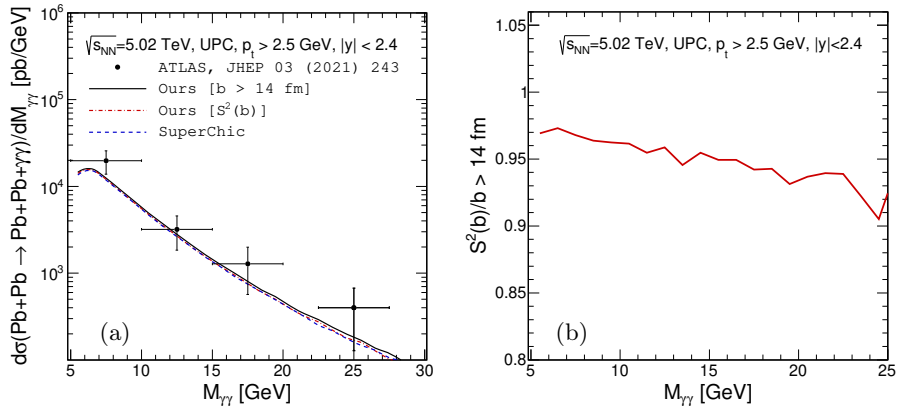

Fig. 4. Differential cross section as a function of diphoton invariant mass at $\sqrt{s_{NN}} = 5.02$ TeV. (a) The ATLAS experimental data are shown together with theoretical results including a sharp cut on impact parameter ($b > 14$ fm (solid black line)) and the smooth nuclear absorption factor $S^2(b)$ (dash-dotted red line). Results obtained from SuperChic [10] are also shown for comparison. The ratio of cross sections for the smooth to sharp cut-off is shown in panel (b).

A planned forward detector for the ALICE experiment — FoCal will start collecting data since Run 4 [11]. Kinematical cuts for photons were applied to take advantage of the lower threshold for photon transverse energy ($E_{t,\gamma} > 200$ MeV) and the accessibility of larger photon rapidity interval ($3.4 < y_{\gamma_{1/2}} < 5.8$). The distribution of diphoton mass is presented in Fig. 5. In this low-mass region, the background from the $\pi^0\pi^0$ production becomes significant. However, using the isotropic distribution of photons in each π^0 decay and imposing a condition of two photons in the experimental acceptance, one can suppress the background. Hence, a cut for vector asymmetry $A_V = |\vec{p}_{t,1} - \vec{p}_{t,2}|/|\vec{p}_{t,1} + \vec{p}_{t,2}|$ was proposed. The implied cut notably reduces the measured cross section for the $\pi^0\pi^0$ background.

From a theoretical perspective, the ALICE-3 experiment presents further opportunities for observation of light-by-light scattering in a new kinematical region. The calculations of cross sections were prepared based on the char-

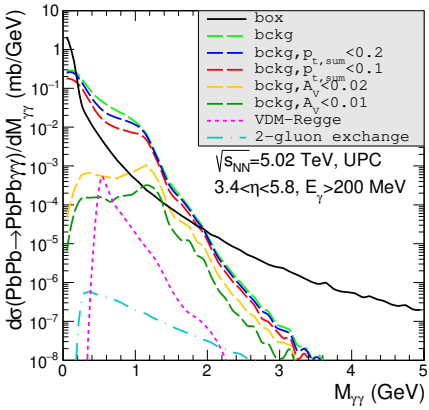

Fig. 5. Invariant mass distribution for the nuclear process. Shown are predictions for the future FoCal acceptance $E_{\mathrm{t},\gamma} > 200$ MeV and $3.4 < y_{\gamma_{1/2}} < 5.8$.

acteristics of the detector including kinematical limitations [12]. Figure 6 shows the diphoton mass distribution in the assumed kinematical range. In the diphoton mass region below 1 GeV the most significant signal comes from the mesonic resonances. The peaks from π^0, η, and η' overachieve even the box contribution, which will allow to observe this contribution for the first time. Here, the impact of the background can be reduced using cuts on $p_{\mathrm{t,sum}}$ or on so-called vector asymmetry.

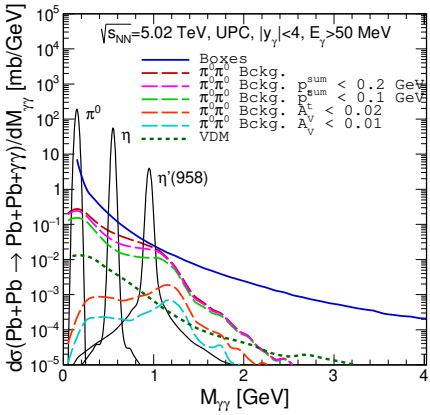

Fig. 6. (Colour on-line) Diphoton invariant mass distribution for ALICE-3, *i.e.* $y_{\gamma_{1/2}} \in (-4, 4)$ and photon energy $E_\gamma > 50$ MeV. Here, the black solid line represents the light-meson resonances, the blue/grey solid line relates to the box contribution, the black dotted line to the VDM-Regge component, and the dashed lines are for the double-π^0 background contribution.

The most challenging task would be a measurement of the VDM-Regge mechanism. Presented in Fig. 3 cross-section distribution shows that the scattered photons in the VDM-Regge process are mainly forward/backward. This fact implies that the dedicated experiment has to have a broad range of photon rapidities. Figure 7 presents a two-dimensional rapidity distribution of (a) box continuum, (b) VDM-Regge mechanism. The red squares represent the coverage of rapidity ranges of the ALICE-3 barrel ($-1.6 < y_{\gamma_{1/2}} < 4$) and forward ($3 < y_{\gamma_{1/2}} < 5$) detectors. This plot reveals that current and planned experiments avoid the region of interest.

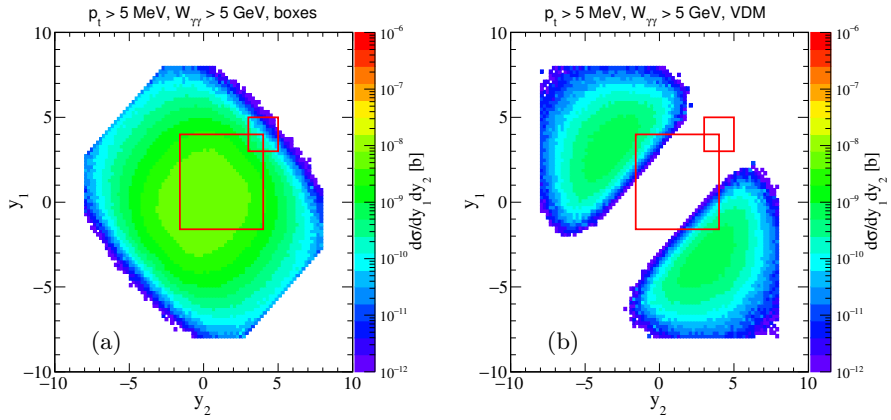

Fig. 7. Distribution in $(y_{\gamma_1}, y_{\gamma_2})$ [in b] for transverse momenta $p_{\mathrm{t},\gamma} > 5$ MeV, di-photon invariant mass $M_{\gamma\gamma} > 5$ GeV. (a) Boxes, (b) VDM-Regge mechanism.

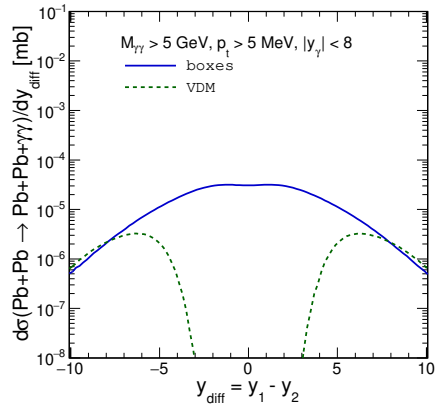

Fig. 8. (Colour on-line) Distribution in y_{diff} for light-by-light scattering processes in PbPb $\to$ PbPb$\gamma\gamma$. Here, the transverse momentum cut is equal to 5 MeV only. The blue solid line relates to the boxes, and the green dotted line to the VDM-Regge contribution. Here, the range of measured diphoton invariant mass is $M_{\gamma\gamma} > 5$ GeV.

However, the introduction of a new variable — the rapidity difference, may facilitate this observation. Figure 8 displays the distribution of the fermionic loops and the VDM-Regge mechanism in the mentioned variable. For the higher values of $|y_{\rm diff}|$, the chances for observing the VDM-Regge mechanisms increase.

5. Conclusion

The future development of new photon detectors opens up new opportunities for light-by-light scattering measurements. The lower threshold of diphoton mass should enable observation of light mesonic resonances. In recent studies, also the method of reduction of the background from the $\pi^0\pi^0$ decays was discussed. The goal of future experimental measurements should be the observation of the VDM-Regge mechanism, not observed so far. However, the required range of measured photon rapidity is difficult to achieve. Also, negative interference of the fermionic loops and the VDM-Regge mechanism generates additional difficulties.

A.S. is indebted to Mariola Kłusek-Gawenda for collaboration on the issues presented here.

REFERENCES

[1] ATLAS Collaboration (M. Aaboud *et al.*), *Nature Phys.* **13**, 852 (2017).
[2] CMS Collaboration (A.M. Sirunyan *et al.*), *Phys. Lett. B* **797**, 134826 (2019).
[3] ATLAS Collaboration (G. Aad *et al.*), *Phys. Rev. Lett.* **123**, 052001 (2019).
[4] P. Jucha, M. Kłusek-Gawenda, A. Szczurek, *Phys. Rev. D* **109**, 014004 (2024).
[5] M. Kłusek-Gawenda, A. Szczurek, *Phys. Rev. C* **82**, 014904 (2010).
[6] T. Hahn, M. Pérez-Victoria, *Comput. Phys. Commun.* **118**, 153 (1999).
[7] M. Kłusek-Gawenda, P. Lebiedowicz, A. Szczurek, *Phys. Rev. C* **93**, 044907 (2016).
[8] M. Kłusek-Gawenda, R. McNulty, R. Schicker, A. Szczurek, *Phys. Rev. D* **99**, 093013 (2019).
[9] M. Kłusek-Gawenda, A. Szczurek, *Phys. Rev. C* **87**, 054908 (2013).
[10] L.A. Harland-Lang, M. Tasevsky, V.A. Khoze, M.G. Ryskin, *Eur. Phys. J. C* **80**, 925 (2020).
[11] ALICE Collaboration (C. Loizides, W. Riegler), CERN Document Server, 2020, CERN-LHCC-2020-009.
[12] ALICE Collaboration (L. Musa, W. Riegler), arXiv:2211.02491 [physics.ins-det].